Journal of Magnetic Resonance 198 (2009) 183–187

Contents lists available at ScienceDirect

Journal of Magnetic Resonance

journal homepage: www.elsevier.com/locate/jmr

Energy efficient iron based electronic field cycling magnet

Dirk Plendl [a], Marian Fujara [b], Alexei F. Privalov [a,*], Franz Fujara [a]

[a] Institut für Festkörperphysik, TU Darmstadt, Hochschulstraße 6, 64289 Darmstadt, Germany
[b] Institut fur Produktionsmanagement, Technologie und Werkzeugmaschinen, TU Darmstadt, Petersenstraße 30, 64287 Darmstadt, Germany

ARTICLE INFO

Article history:
Received 5 December 2008
Revised 6 February 2009
Available online 20 February 2009

Keywords:
NMR
Electronic field cycling
Magnet design
Spin-lattice relaxation dispersion

ABSTRACT

A new concept for an energy efficient electromagnet for fast field cycling NMR applications as well as its construction and first test results are presented. The magnet, which provides a rectangular sample space of 17 × 25 mm, has an iron yoke and pole pieces optimised with respect to the B_0 homogeneity. The maximum field is 0.66 T at a current of 320 A; its field inhomogeneity for a cylindrical sample (length 7 mm, diameter 6 mm) is about 50 ppm. The power dissipation during polarisation at 0.55 T is as low as 1.4 kW. The magnet is powered by a commercially available power supply and can be rapidly switched with a slew rate of 0.55 T/ms. The system has shown a stability of 50 ppm/h.

1. Introduction

Field-cycling (FC) NMR is an established method for the investigation of field dependent nuclear spin phenomena, like relaxation dispersion, polarization transfer, enhanced NQR etc. [1,2]. In an FC experiment the magnetic field is switched rapidly among several distinct levels where the spin ensemble evolves. The signal detection is always performed at the maximum magnetic field. This allows for investigations over a wide range of field strengths, ranging from almost zero, without changing the spectrometer setup and preserving the sensitivity typical for high field NMR.

Several realizations of fast FC have been published[1]: mechanical [3–5] and electronical [6–8] FC.

The highest slew rates of 0.55 T/ms can be achieved with electronic FC where the field is varied by rapidly changing the current fed into an electromagnet. The electromagnet is specially optimized for FC as it should enable fast switching as well as a high maximum field of reasonable homogeneity.

Today, most FC magnets in use, home built or a commercial product of STELAR [9], are resistive air core coils. These systems are very energy consuming and require powerful cooling systems because of the high energy density in the coil. This is a problem which arises from the following: fast switching is favored by low inductance L. Low inductance is achieved by reducing the energy stored in the effective coil volume, i.e. building a small air core coil with only very few windings. On the other hand a strong magnetic field with good homogeneity requires high current densities, many windings and a large coil volume.

All these requirements contradict each other, thus enforcing some compromises. Moreover, energy dissipation has to be kept in mind, since the field strength is ultimately limited by the amount of heat that can be extracted by the cooling system.

The complexity of a conventional FC spectrometer results to a considerable degree from its high energy consumption. This affects two parts: the power supply (tens of kW) and the proper cooling system. Both are cost and space consuming, thus rendering modern field cycling a rarely used method.

In this work we describe a novel design of a FC magnet with reduced energy consumption and significantly lower operating costs. This system operates with a commercially available current source and is much less involved in cooling and protection.

Unlike other systems, it uses iron for field magnification, thus generating a stronger field at a given current and reducing the overall energy consumption.

2. Design and optimization

The magnet described in this work is basically a dipole magnet depicted in Fig. 1. The field is generated by an iron yoke that is magnetized by two coils. Pole pieces are used for shaping the field in the air gap to gain the best possible field homogeneity.

The pole pieces were designed using a scalar potential approach [10,11]. In this method the magnetic field in the air gap is described by a scalar potential which is an analytical function depending on a set of paramters. By varying these parameters, one can construct a field of the desired homogenity. The shape of the pole pieces can then be deduced from the scalar potential.

* Corresponding author.
E-mail address: alexei.privalov@physik.tu-darmstadt.de (A.F. Privalov).

[1] The given set of references does not cover the entire available literature but rather refers to some important recent concepts. Further references are found therein.

1090-7807/$ - see front matter © 2009 Elsevier Inc. All rights reserved.
doi:10.1016/j.jmr.2009.02.004

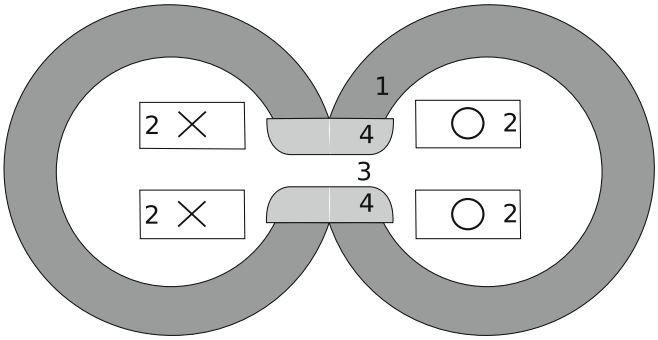

Fig. 1. Magnet cross section: (1) iron yoke, (2) coils, (3) air gap for sample, (4) pole pieces.

In a region near the air gap, without currents ($\nabla \times \vec{B} = 0$) the magnetic field can be described by a scalar potential Φ:

$$\vec{B} = \nabla\Phi \tag{1}$$

which is a solution of the Laplace equation

$$\Delta\Phi = 0. \tag{2}$$

To construct a pair of rotationally symmetric pole pieces, we use cylindrical coordinates (ρ,ϕ,z) with z being the direction of the magnetic field and the sample located at the origin.

By searching for solutions which are products of functions of one coordinate each,

$$\Phi(\rho, \phi, z) = R(\rho)Q(\phi)Z(z) \tag{3}$$

and setting Q = const. we find

$$\Phi(\rho, z) = (a\sinh(kz) + b\cosh(kz))J_0(k\rho) \tag{4}$$

with J_0 denoting the Bessel functions of the first kind of order zero and a,b,k being arbitrary constants.

The corresponding magnetic field can be calculated as

$$B_z(\rho, z) = k(a\cosh(kz) + b\sinh(kz))J_0(k\rho). \tag{5}$$

The first term describes a field which is approximately constant in the vincity of the origin whereas the second term describes a field with a linear z gradient. We therefore set $b = 0$.

As the Laplace equation is linear, we can construct a more general solution as a superposition of many base functions:

$$\Phi(\rho, z) = \sum_{i=1}^{N} a_i \sinh(k_i z)J_0(k_i\rho) \tag{6}$$

The optimization goal was to obtain a constant field in a sample volume around the origin having a height of 5 mm and a radius of 7 mm. The quality of the field was measured by the mean square deviation σ^2 of the field at certain points from a predefined value B_0[2]

$$\sigma^2 = \frac{1}{N}\sum_{i=1}^{N}(B(\vec{r}_i) - B_0)^2 \tag{7}$$

The points $\vec{r}_i$ were chosen at z=0 mm and ρ_i = 0, 2, 4 and 6 mm. To limit the pole pieces radius, an additional point was added at ρ = 40 mm and set to B=0.

The optimization was performed with N = 5 base functions and the parameters a_i and k_i were selected for best homogeneity. The minimization was carried out with Mathematica and a field with an inhomogeneity of 40 ppm over 0.75 cm^3 was found.

Once a sufficiently homogeneous field is obtained, pole pieces providing this field can be built by shaping the surface of a highly permeable material according to an equipotential surface. This is possible since magnetic flux lines are always normal to the surface of a high permeable material.

[2] The exact value of B_0 is not important for the optimization process as the field strength and its spatial dimensions can be arbitrarily changed by scaling factors.

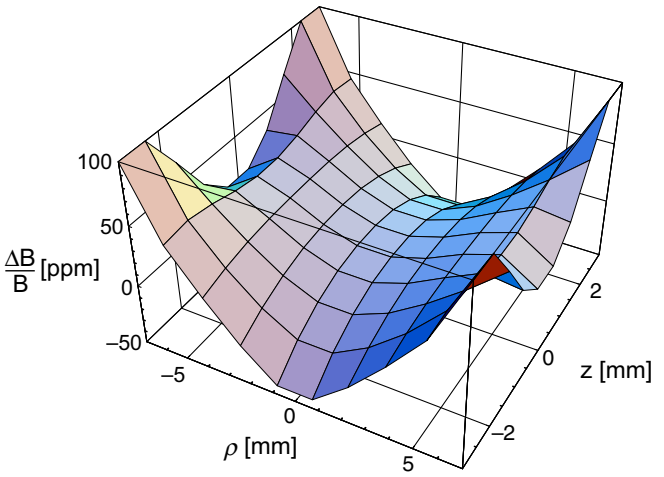

Fig. 2. Calculated field profile in the (ρ,z)-plane (with z being the symmetry axis), relative deviation of the field from its value at the center in ppm.

The pole contour $z(\rho)$ was calculated by numerically solving

$$\Phi(\rho, z(\rho)) = \Phi(0, \delta/2) \tag{8}$$

with δ = 17.4 mm as the gap between the pole pieces at the center.

The quality of the analytically optimized field was examined using finite-element programs. It turned out that the analytically and numerically calculated fields were only in good agreement for a very high permeable material (e.g. μ = 10,000) and for small gaps ($\delta \leqslant 8$ mm). As the magnet has a gap height of 17.4 mm, the pole contour was further optimized: a small correcting function $c(\rho) = c_1\rho^2$ was superimposed to the analytical pole piece contour and numerically optimized for the most homogeneous field. A profile of the final field with a homogeneity of 150 ppm over a volume of 0.75 cm^3 is shown in Fig. 2.

3. Construction

The yoke and the assembled magnet are shown in Fig. 3. Construction and material choices are described in the following for the most important parts.

3.1. Yoke

The yoke consists of four rings of a highly permeable iron alloy (Vitroperm 500F, Vacuumschmelze GmbH, Germany). These rings are made of thin isolated metal slices. The isolation prevents the induction of eddy currents during switching. Vitroperm 500F is a very soft magnetic material having a small hysteresis, but its saturation field strength of 1.2 T sets an upper bound for the magnetic field strength. The rings have an inner diameter of 110 mm, an outer diameter of 160 mm and a thickness of 25 mm.

In each ring a gap of 50 mm height is cut, leaving room for the pole pieces. The cut surface was stabilized by epoxy resin. The rings are fixed by two plates of PVC with proper indentations holding them in position. The plates are pressed to each other by brass screws.

3.2. Pole pieces

The pole pieces are those parts with the largest influence on field homogeneity. Therefore, precise machining and exact alignment is crucial for the performance of the magnet. To minimize eddy currents the pole pieces are made of a nonconductive iron

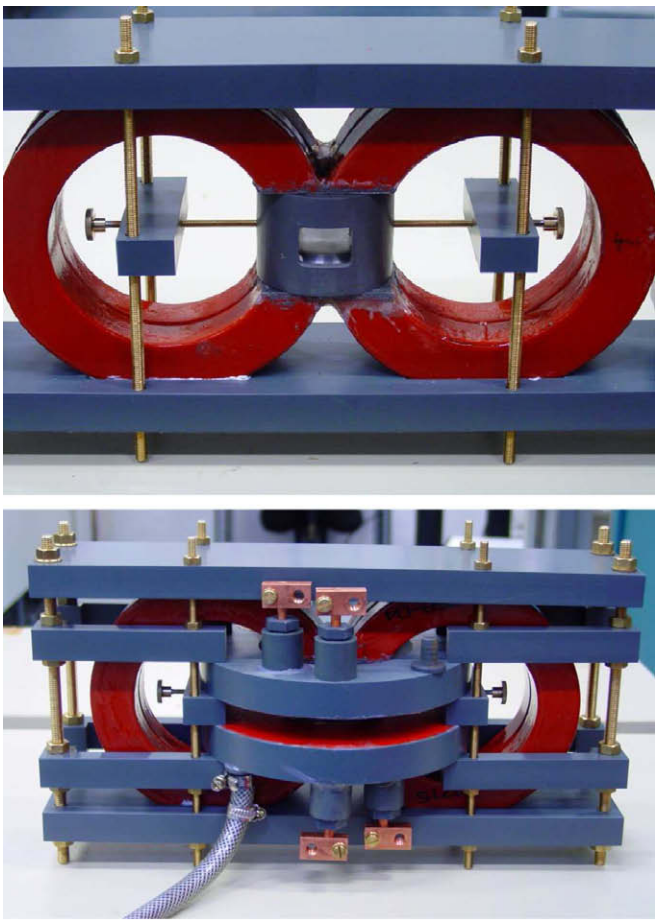

Fig. 3. Pole pieces, yoke and space (top) and the whole magnet (bottom).

powder material, milled from a cylindric raw part. A simultaneous five-axes machining process is used to minimize form errors to the ideal shape. The numerical control program of the tool path is generated by computer aided manufacturing software, using a machining strategy that keeps the orientation angles between tool and workpiece constant. This ensures a constant effective cutting speed as required for a smooth surface finish. A ball-type milling tool was used for roughing and finishing operations. To achieve a constant kinematic roughness, the width of cut is adapted to the curvature of the pole piece. The maximum form error is below 3 μm. The dimensions of the pole pieces are 60 mm in diameter and 16 mm in thickness.

The pole pieces have to be aligned precisely to get the desired field homogeneity. Numerical simulations showed that the most severe loss in field homogeneity is caused by a tilt of the pole pieces. Therefore their surfaces have to be parallel with an accuracy of better than 10 μm.

For this purpose the pole pieces are mounted and glued onto a special spacer, which holds them apart at a distance of 17 mm. The spacer is a cylindrical PVC piece with two cavities from the opposite sides for each pole piece. The cavities are turned from the same side of the work piece without loosening it from the lathe making both surfaces as parallel as possible. Finally a slot of 17 mm $\times$ 25 mm was cut through the center of the spacer, giving access to the homogenous field region for the NMR probe.

3.3. Coils

The magnet is powered by two identical coils each having 30 turns of isolated copper wire. The coils are connected in series.

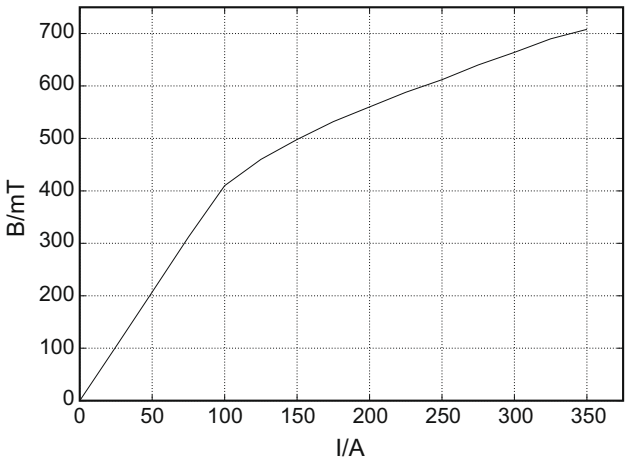

Fig. 4. Magnetic field at sample position depending on current.

The available space for the coils allowed us to use four 2 mm thick copper wires in parallel resulting in a total resistance of 35 mΩ. The coils were wound in parallel on a bobbin, stabilised with glue and mounted in the closed PVC housing. The dimensions of the housing are: 180 mm outer diameter, 80 mm inner diameter and 23 mm height. A solution with several conductors in parallel renders winding less complicated and increases the cooling surface of the conductor. Isolation of wires allows using water as a coolant. The coolant flow is 0.1 l/s at a preasure of 0.5 bar. The cooling efficiency was tested at a continuous current of 200 A, resulting in a dissipated energy of 1400 W and a temperature increase in the wire of about 11 K.

3.4. Power supply

The magnet is powered by a Copley 266 (Copley Controls Corp., Canton, USA) amplifier acting as a controlled current source. It can deliver a continuous current of 250 A and a peak current of more than 350 A. It is controlled by a 20 Bit DAC delivering a current resolution of ±1 mA.

4. Tests

For field measurements we used a calibrated Hall probe FM210 (Projekt Elektronik GmbH, Berlin).

Additional NMR tests were performed on a home built single-channel spectrometer using the specialised DAMARIS control software [12].

4.1. Linearity

The current dependence of the magnetic field is shown in Fig. 4. Below 100 A the field grows almost linearly in agreement with Eq. (A.4) (Appendix A). Above 100 A, the slope of the curve decreases. At 225 A, the field reaches only 0.58 T instead of estimated 1 T (see Eq. (A.4)). The reason for this disagreement is probably the saturation of the yoke. Especially the cross section may be underdimensioned.

4.2. Hysteresis

The maximum hysteresis (uncertainty in field strength) is ±1 mT at 0.3 T (see Appendix B). This small error becomes significant for low evolution fields (below 50 kHz) and should be compensated for.

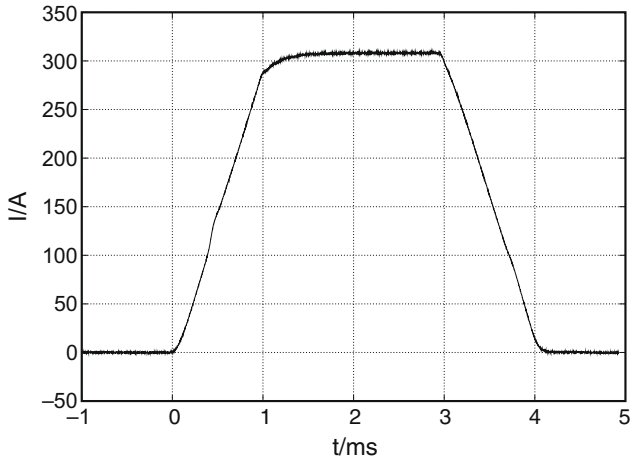

Fig. 5. Switching a current of 310 A.

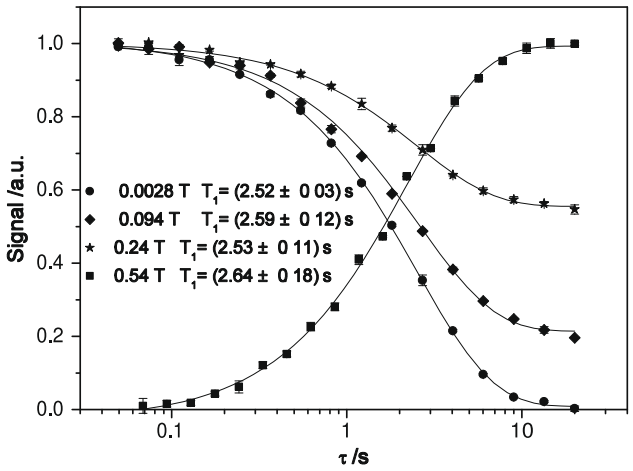

Fig. 7. Magnetisation decay curves of a water sample for various evolution fields given in the insert. The curves were fitted individually yielding spin-lattice relaxation times also given in the insert.

At the beginning of most FC experiments, a strong magnetic field is applied to the sample. This strong magnetic field also polarizes the magnet iron nearly to saturation, so that the magnet is in a well defined state. We therefore assume that the switching to the lower evolution field will result in reproducible field levels.

We use the measured field strength curve as the calibration of the system and thus compensate for the nonlinearity of the coil, the possible nonlinearity of the amplifier and the hysteresis.

4.3. Switching time

The applied amplifier has the advantage of fast bipolar switching applying a very high voltage of ±350 V. The field switching time is presented in Fig. 5. As can be seen, switching a current of 310 A on or off lasts about 1.2 ms, corresponding to a slew rate of about 0.55 T/ms. Additionally, one has to wait about another ms, depending on the PID controller, for the field to become stable. In normal use, the total switching time (from the beginning of switching until reaching a stable field) is 2 ms.

4.4. NMR tests

The field homogeneity was tested by observing the ^{1}H NMR line width of three different water samples. The spectra (Fig. 6) give the field distribution in the sample volume. The inhomogeneity can be described by the ratio of the full width at the half-height with respect to the NMR frequency. For the smallest sample, a sphere of 4 mm diameter, it is 25 ppm, for the largest, a cylinder with a length of 7.5 mm and a diameter of 6 mm it is 52 ppm.

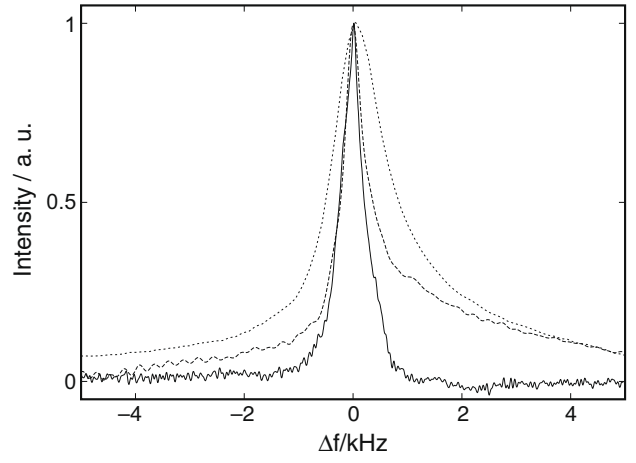

Fig. 6. Line shapes for water samples at 27 MHz: solid line, a sphere of 4 mm diameter; dashed line, a cylinder of 5 mm length and 4 mm diameter; dotted line, a cylinder of 7.5 mm length and 6 mm diameter.

The stability of the system was estimated by observing the frequency drift of the water NMR spectral line over a series of experiments. These drifts were typically in the range of ±1 kHz during several minutes of continuous pulsing. The thermal drift after longer polarization times has a comparable value of ±1 kHz and it is essentially determined by the stability of the power amplifier. The thermal drift of the magnet itself is even weaker.

The reproducibility is quite acceptable, allowing us to accumulate signals from individual channels (quadrature detection) instead of using power amplitudes. Several magnetization decay curves from a water sample of 5×4 mm^2 are presented in Fig. 7 for various evolution fields.

5. Conclusion

After construction and numerous test runs we are confident that an iron based magnet is well applicable for fast field cycling. The advantages of this design are: several times lower energy consumption as well as less sophisticated cooling and protection if compared to air core magnet designs for comparable magnetic fields. Low energy consumption permits the use of a commercial current amplifier. This allows for a switching with comparatively high voltage of 350 V, thus keeping the switching times in the millisecond range in spite of a comparatively high inductance of 1.2 mH. The homogeneity, short and long term stability of the system are quite acceptable for field cycling relaxometry and well competitive with air core systems.

As a disadvantage we note the necessity of a precise field calibration to avoid nonlinearitys and hysteresis effects.

Acknowledgments

We thank the mechanical workshop of the Institut für Festkörperphysik for machining the components of the magnet, H. Plößer for his advice on numerous construction details and CST GmbH for providing an academic version of the 3D magnetic field simulation software CST EM STUDIO.

Appendix A. Dimensioning of the coils

The magnetic field in the air gap can be calculated from Ampere's Law

$$\oint Hds = \int jdA \tag{A.1}$$

which states that the integral of the magnetizing field H around a closed loop equals the total current that flows across the loop. For a coil consisting of many turns, the total current NI is the product of the current I and the number of turns N. Given the magnetizing field inside iron and air gap we can calculate the current:

$$NI = H_{\text{iron}} l + H_{\text{air}} \delta \tag{A.2}$$

with l denoting the length of the yoke and δ the width of the air gap. The magnetic field B and the magnetizing field H are connected by the material permeability: $B = \mu_0 \mu H$

$$NI = \frac{B_{\text{iron}} l}{\mu_0 \mu} + \frac{B_{\text{air}} \delta}{\mu_0} \tag{A.3}$$

Assumeing that the magnetic field strength is approximately constant over the magnet, we put $B_{\text{iron}} = B_{\text{air}} = B$ and

$$NI = \frac{B}{\mu_0}\left(\frac{l}{\mu} + \delta\right) \tag{A.4}$$

For nonsaturated iron the permeability is large and the current only depends on the gap size and the field strength.

Appendix B. Field reproducibility

Due to the iron hysteresis, the magnetic field is not uniquely determined by the current. The size of this uncertainty can be estimated by calculating the remanent field strength B_r. Solving Eq. (A.2) for zero current and inserting the iron coercitivity field, H_c, we get:

$$B_r = -\mu_0 H_c \frac{l}{\delta} \tag{B.1}$$

which shows that with magnetically soft material ($H_c = 3$ A/m for the yoke, $H_c = 390$ A/m for the pole pieces), the remanent field is of the order of 1 mT.

References

[1] F. Noack, Progr. NMR Spectrosc. 18 (1986) 171.
[2] R. Kimmich, E. Anoardo, Progr. NMR Spectrosc. 44 (2004) 257.
[3] S. Swanson, S. Kennedy, J. Magn. Reson. 102 (1993) 375.
[4] S. Grosse, A.V. Yurkovskaya, J. Lopez, H.-M. Vieth, J. Phys. Chem. A 105 (26) (2001) 6311.
[5] H. Stork, M. Ditter, H. Plößer, A.F. Privalov, F. Fujara, J. Magn. Reson. 192 (2008) 173–176.
[6] K.-H. Schweikert, K. Krieg, F. Noak, J. Magn. Reson. 78 (1988) 77.
[7] M. Blanz, T. Rayner, J. Smith, Meas. Sci. Technol. 4 (1993) 48.
[8] O. Lips, A.F. Privalov, S. Dvinskikh, F. Fujara, J. Magn. Reson. 149 (2001) 22–28.
[9] STELAR s.n.c, Mede (Italy), Spimaster FFC. Available from: <http://www.stelar.it/>.
[10] P.M. Glover, P.S. Aptaker, J.R. Bowler, E. Ciampi, P.J. McDonald, J. Magn. Reson. 139 (1999) 90.
[11] A.E. Marble, I.V. Mastikhin, B.G. Colpitts, B.J. Balcom, J. Magn. Reson. 174 (2005) 78.
[12] A. Gädke, M. Rosenstihl, C. Schmidtt, H. Stork, N. Nestle, Diffusion Fundamentals 5 (2007) 6.1. Available from: <http://www.fkp.physik.tu-darmstadt.de/damaris/>.